

# Experiment M8

## **Lifetime of positrons in matter**

Laboratory class particle physics, RWTH Aachen University

July 2013

### **Prerequisites**

- Basic knowledge of the characteristics and decay of positronium
- Measurements with scintillation counters
- Coincidence electronics
- Fast pulse electronics

### **Aim of the experiment**

- Determination and comparison of the lifetimes of positrons in polyethylene and aluminium.
- Determination of the relative fraction of the formation of positronium in polyethylene.

### **Method**

For the measurement of the lifetime, a time spectrometer for times in the ns-regime is used. For this, the 1.28 MeV  $\gamma$ -transition from the decay of the positron emitter  $^{22}\text{Na}$  is used as the start signal, and one of the annihilation photons, caused by the decay of the positron in matter, is used as the stop signal.

## Contents

<b>1</b>	<b>Decay of a <math>e^+e^-</math>-pair</b>	<b>1</b>
1.1	Stopping of positrons . . . . .	1
1.2	The modes of $e^+e^-$ -decay . . . . .	2
1.3	Selection rules for the $e^+e^-$ -decay . . . . .	3
<b>2</b>	<b>Positron states in matter</b>	<b>4</b>
2.1	The “Øre-gap” theory of positronium formation . . . . .	4
2.2	The $^3S \rightarrow ^1S$ conversion . . . . .	5
<b>3</b>	<b>Experimental setup</b>	<b>5</b>
3.1	Source and detector . . . . .	5
3.2	The time spectrometer . . . . .	6
3.3	Operating point and calibration of the setup . . . . .	7
<b>4</b>	<b>Analysis of the time spectra</b>	<b>8</b>
4.1	The “tail” method . . . . .	9
4.2	The “centroid shift” method . . . . .	9
<b>5</b>	<b>Experimental procedure</b>	<b>10</b>
5.1	Setting up, adjusting of the operating point and calibration . . . . .	10
5.2	Measurement series . . . . .	11
<b>6</b>	<b>Analysis and report</b>	<b>12</b>
<b>A</b>	<b>Devices and material</b>	<b>12</b>
A.1	Devices . . . . .	12
A.2	Material . . . . .	13

## References

- [1] W.R. Leo: Techniques for Nuclear and Particle Physics Experiments, Second Revised Edition, Springer Verlag 1994, ISBN 3540572805
- [2] J. Chang: Table of Nuclides, KAERI (Korea Atomic Energy Research Institute), <http://atom.kaeri.re.kr/ton/>, Stand: 30.7.2010
- [3] T. Kohonen: Contributions to the study of life times of positrons in solids, Annales Academiae Scientiarum Fennicae, Ser. A, Vol. VI: Physica, No. 92 (1961) S. 1–79
- [4] H. Neuert: Kernphysikalische Meßverfahren zum Nachweis für Teilchen und Quanten, Verlag G. Braun, Karlsruhe 1966, Signatur der Physikbibliothek: Dr 129
- [5] National Nuclear Data Center: Chart of Nuclides database, Brookhaven National Laboratory, <http://www.nndc.bnl.gov/chart/>, Stand: 30.7.2010
- [6] G. Otter, R. Honecker: Atome – Moleküle – Kerne, Band I, Atomphysik, 2. Auflage, Teubner Verlag 1998, ISBN 3519132192, Signatur der Physikbibliothek: 1<sup>1</sup> Bo 184 (1. Auflage, 1993)
- [7] R. N. West: Positron studies of condensed matter, Advances in Physics, Volume 22, Issue 3 May 1973, S. 263–383, DOI: 10.1080/00018737300101299, <http://dx.doi.org/10.1080/00018737300101299>, Signatur der Physikbibliothek: 22 Z 5
- [8] B. Williams: Positron-Annihilation, in: Compton Scattering: Tool for the Investigation of Electron Momentum Distribution, McGraw-Hill Inc., New York 1977, ISBN 0070703604, Signatur der Physikbibliothek: Bo 145
- [9] Wikipedia-Artikel: Compton-Effekt, <http://de.wikipedia.org/wiki/Compton-Effekt>, Stand: 27.8.2010

# 1 Decay of a $e^+e^-$ -pair

## 1.1 Stopping of positrons

Positrons in matter are mostly stopped, before they annihilate with an electron (see section 1.2). The time needed for the stopping can in principle be determined from the Bethe Formula. The stopping time  $dt$  per energy loss  $dE$  is given by

$$\frac{dt}{dE} = \frac{\frac{dt}{dx}}{\frac{dE}{dx}} = \frac{1}{v \cdot \frac{dE}{dx}}. \quad (1)$$

The energy loss occurs through collisions with shell electrons. Under consideration of the  $e^+e^-$  scattering cross section<sup>1</sup>, theory produces the formula for the slowing down to kinetic energies in the order of 10 keV [3]:

$$\frac{dt}{dE} = \frac{m_e (4\pi \epsilon_0)^2}{2\pi e^4 N Z} \frac{v(E)}{\ln\left(\frac{E^2 \gamma + 1}{I^2 \frac{\gamma + 1}{2}}\right) + f(\gamma)} \quad (2)$$

- with  $E$  total energy of the positron ( $= \gamma \cdot m_e c^2$ )  
 $v(E)$  velocity of the positron  
 $\gamma$  Lorentz factor of the positron ( $\gamma = 1/\sqrt{1 - \beta^2}$ ,  $\beta = \frac{v}{c}$ )  
 $m_e$  mass of the positron/electron  
 $N$  atomic density of the medium  
 $Z$  charge number of the medium  
 $I$  mean excitation energy of the medium ( $I \approx 13.4 \text{ eV} \cdot Z$  for light elements)  
 $f(\gamma) = 2 \ln 2 - \frac{\beta^2}{12} \cdot \left(23 + \frac{14}{\gamma + 1} + \frac{10}{(\gamma + 1)^2} + \frac{4}{(\gamma + 1)^3}\right)$

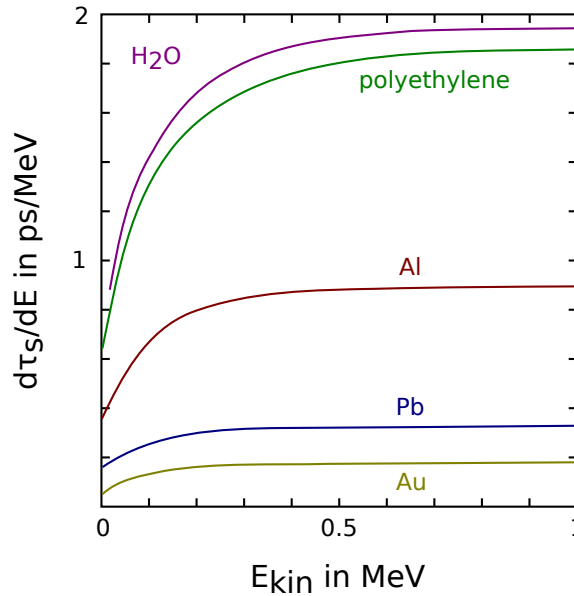


Figure 1: Differential stopping time for various materials as a function of the kinetic energy of the positron

In figure 1 the function is shown for some materials. For the positrons produced by  $^{22}\text{Na}$ , with a mean kinetic energy of 180 keV, the following times for slowing down can be calculated:

material	$\tau_s$ [ps]
H <sub>2</sub> O	0.24
polyethylene	0.22
aluminum	0.11
lead	0.048

<sup>1</sup>Bhabha scattering

In the range between 10 keV and 100 eV the following approximation [3] can be used:

$$\tau_s = \sqrt{\frac{eV}{E}} \cdot 10^{-16} \text{ s}, \quad (3)$$

where  $E$  is the final kinetic energy. This means an additional slow down time of  $10^{-17}$  s.

In metals the further stopping down to thermal energies ( $\approx 0.025$  eV) takes around 3 ps. The stopping in metals therefore takes only a few pico seconds in total. Therefore it can be assumed that positrons in metals annihilate primarily at thermal energies.

In isolating crystals the thermalization takes significantly longer, because no free electron states are available for the absorption of energy. Here the energy transfer has to happen through the excitation of lattice vibrations (phonons). Theory predicts a value in the order of 300 ps for the thermalization. This is already in the order of the mean lifetime of para-positronium<sup>2</sup>. Therefore it is possible for positrons to annihilate in isolating crystals before thermalization.

In amorphous materials (plastics, etc.) significantly shorter stopping times are expected because of the multitude of structural irregularities of the medium.

## 1.2 The modes of $e^+e^-$ -decay

The following considerations of possible decay modes of  $e^+e^-$  pairs are based on [7]. During the annihilation of an  $e^+e^-$  pair two or more  $\gamma$  quanta are produced. The production of a single photon is in principle possible, but only if a further partner (atom or ion) is involved to balance the momentum. In the usual experiments with positrons this process is irrelevant.

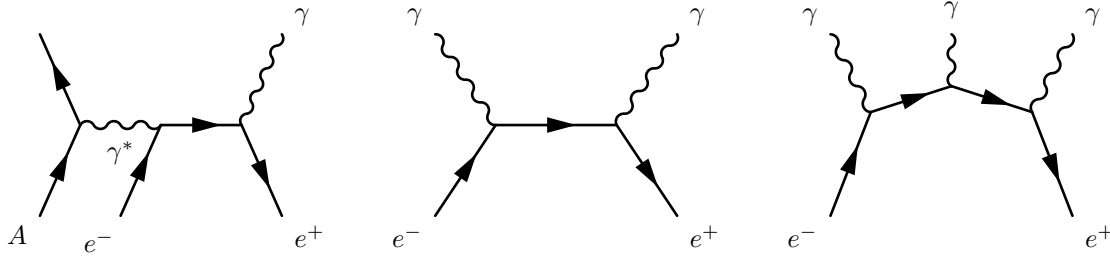


Figure 2: Feynman graphs for the  $e^+e^-$  annihilation into one, two and three  $\gamma$  quanta

**Task 1:** Calculate the energies and momenta of the two or three photons from the annihilation of positron and electron in the center of mass system!

Figure 2 shows the Feynman graphs for the annihilation into one, two and three photons. The cross sections follow roughly:

$$\frac{\sigma_{1\gamma}}{\sigma_{2\gamma}} \approx \alpha^4, \quad \frac{\sigma_{3\gamma}}{\sigma_{2\gamma}} \approx \alpha, \quad (4)$$

where the fine-structure constant  $\alpha = \frac{e^2}{4\pi\epsilon_0\hbar c}$  is approximately  $\frac{1}{137}$ .

The process of lowest order in  $\alpha$  is the decay into two  $\gamma$ . The cross section for unpolarized positrons with a free electron at rest for the relativistic case is:

$$\sigma_{2\gamma} = \alpha^2 \lambda_c^2 \frac{\pi}{\gamma + 1} \left( \frac{\gamma^2 + 4\gamma + 1}{\gamma^2 - 1} \ln(\gamma + \sqrt{\gamma^2 - 1}) - \frac{\gamma + 3}{\sqrt{\gamma^2 - 1}} \right) \quad (5)$$

with  $\lambda_c = \lambda_c/2\pi$

$\lambda_c = h/m_e c$  Compton wavelength of the electron<sup>3</sup>

For the non-relativistic case this relation can be approximated to:

$$\sigma_{2\gamma} \approx \frac{\pi \alpha^2 \lambda_c^2}{\beta} \quad (6)$$

<sup>2</sup>see section 2

<sup>3</sup>see also [6, Chapter 1]

Because  $\sigma_{2\gamma}$  is Lorentz-invariant, this equation also holds for the case that electron and positron are traveling in a medium<sup>4</sup>. The probability  $\lambda_{2\gamma}$  for the annihilation of the photon per time unit is then:

$$\frac{1}{\tau_{2\gamma}} = \lambda_{2\gamma} = 4 \sigma_{2\gamma} \cdot n_e \cdot v = 4\pi \alpha^2 \cdot \lambda_c^2 \cdot c \cdot n_e \quad (7)$$

with  $n_e$  electron density  
 $\tau_{2\gamma}$  mean lifetime of the positrons

The factor of 4 is a spin-weighting factor, resulting from the averaging and summation over the possible spins in the initial and final states.

According to that, the mean lifetime of the positrons in a medium is proportional to the inverse electron density, but independent of the velocity of the positrons.

The decay into three  $\gamma$  quanta is described by quantum-electrodynamics in its non-relativistic approximation, averaged and summed over all spin and polarization states:

$$\sigma_{3\gamma} = \frac{4}{3} \frac{\alpha^3 \lambda_c^2}{\beta} (\pi^2 - 9) \quad (8)$$

For the corresponding decay constant a further spin weighting factor  $\frac{4}{3}$  has to be regarded:

$$\frac{1}{\tau_{3\gamma}} = \lambda_{3\gamma} = \frac{4}{3} \sigma_{3\gamma} \cdot n_e \cdot v = \frac{4}{3} \cdot \frac{4}{3} \alpha^3 \lambda_c^2 c n_e (\pi^2 - 9) \quad (9)$$

**Task 2:** Calculate the factor by which the 3- $\gamma$ -decay of the positron is less likely than the 2- $\gamma$ -decay. Use the given formulas.

### 1.3 Selection rules for the $e^+e^-$ -decay

The decay of an  $e^+e^-$  pair occurs from a quantum state with given symmetries. For electromagnetic interactions all symmetries are preserved, that means conservation laws have to be respected. This leads to selection rules for the decay. The deduction can be found in [7].

The ground states of an  $e^+e^-$  pair are the  $^1S$  state (singlet) and the  $^3S$  state (triplet) with antisymmetric and symmetric spin wave functions of the  $e^+$ - and  $e^-$  particles. A bound  $e^+e^-$  pair is a so-called positronium.

Photons have the spin  $j = 1$  with the two states  $j_3 = +1$  or  $j_3 = -1$ .<sup>5</sup> The state  $j = 0$  and  $j_3 = 0$  does not exist for photons. Therefore it is not possible to combine two photons to have a total spin of  $J = 1$ . For this reason the decay into two photons is forbidden for the  $e^+e^-$  triplet state.

An other important symmetry is the charge parity (C-conjugation). For a fermion-antifermion pair it is given by:

$$C = P_i P_l P_s \quad (10)$$

with  $P_i$  internal parity of the pair  
 $P_l$  spatial parity  
 $P_s$  spin parity

$P_i$  is calculated by multiplication from the internal parities of the particles and is  $P_i = -1$  for fermion-antifermion systems.

$P_l$  depends on the quantum number of orbital angular momentum  $l$  and is determined by the symmetry properties of the spherical harmonics for point reflections with respect to the point of origin:

$$P_l = (-1)^l \quad (11)$$

The spin parity  $P_s$  for a fermion-antifermion pair can be found in the table of Clebsch-Gordan coefficients for the combination of particles with spin  $\frac{1}{2}$ :

$$P_s = (-1)^{s+1}, \quad s = \begin{cases} 0 & \text{singlet} \\ 1 & \text{triplet} \end{cases} \quad (12)$$

<sup>4</sup>Here  $\beta = v/c$  is the relative velocity of both partners

<sup>5</sup>Photons with  $j_3 = +1$  are right-handed and therefore left-handed-circular polarized. Photons with  $j_3 = -1$  are called left-handed and the light is called right-handed polarized.

For a  $e^+e^-$  pair it follows:

$$C = (-1)^{l+s} \quad (13)$$

Therefore  $C$  is  $+1$  for the singlet and  $-1$  for the triplet in its ground state.

The charge parity of the photon is  $C = -1$  and for a system of  $n$  photons

$$C_n = (-1)^n. \quad (14)$$

For the electromagnetic interaction the charge parity is conserved. Therefore the singlet state can only decay into an even number of photons and the triplet state can only decay into an odd number of photons.

According to quantum electrodynamics, the possibility for an annihilation into  $n + 1$  photons is in general reduced by a factor of  $\alpha$  compared to that of the decay in  $n$  photons. Therefore it can be assumed, that the  $^1S$  state virtually always decays into two  $\gamma$  quanta, and that the  $^3S$  state only decays into three  $\gamma$  quanta [8].

It is therefore possible to calculate the lifetime of the positronium. In the above formulas for  $\tau_{2\gamma}$  and  $\tau_{3\gamma}$ ,  $n_e = |\psi(0)|^2$  has to be inserted, where  $\psi(r)$  is the wave function of the positronium in its ground state.

**Task 3:** Find the normalized wave function of the ground state of positronium  $\psi(r)$  and calculate the lifetime of both states  $\tau_{2\gamma}$  and  $\tau_{3\gamma}$ . The results should agree roughly with [3], [7], [8].

## 2 Positron states in matter

The spectra of the  $e^+e^-$  lifetimes can have more than one component, depending on the medium. This is caused by the different initial states, from which the positrons can decay. They can decay spontaneously with a free electron into two or three  $\gamma$  quanta. Additionally it may form bound states of  $e^+e^-$  in solid matter, which are called positronium. Here para-positronium (singlet state) and ortho-positronium (triplet state) can be distinguished. The lifetime of these states strongly depends on the structure of the matter. Therefore the measurement of the lifetime of positrons in matter is important for solid state physics.

### 2.1 The “Øre-gap” theory of positronium formation

The formation of positronium is only possible if the initial energy of the positron has to be in a small interval, called the “Øre-Gap” [7], [3]. On the one hand, the positron, together with the binding energy of the positronium, has to provide enough energy to ionize a molecule in the medium and to bind to the electron:

$$E_{min} = E_i - E_B \quad (15)$$

with  $E_i$  ionization energy of a molecule in the medium  
 $E_B = \frac{Ry}{2} \approx 6.8$  eV binding energy of isolated positronium<sup>6</sup>

On the other hand the energy must not be much higher than the first excitation energy  $E_e$  of the molecule. Otherwise the energy of the positron would be lost, because the excitation of the molecule is much more likely than the formation of positronium. This means:

$$E_i - E_B < E < E_e \quad (16)$$

In solid matter with a lattice structure and energy bands, the different affinities have to be taken into account:

$$(E_i + Q_p) - (BE + Q_{pos}) < E < E_1, \quad (17)$$

where  $E_i$  ionization energy = energy to remove an electron from the upper border of the valence band out of the crystal  
 $Q_p$  affinity of the crystal for positrons  
 $Q_{pos}$  affinity of the crystal for positronium  
 $BE$  binding energy of positronium in the matter (can be smaller than  $\frac{Ry}{2}$ )  
 $E_1$  excitation energy into the lowest vacant energy state (= band gap)

When it is considered that  $E_i - E_1 = Q_e$  is the electron affinity, the Øre-Gap only exists if:

$$Q_e + Q_p < Q_{pos} + BE \quad (18)$$

---

<sup>6</sup>Rydberg constant  $Ry = m_e c^2 \alpha^2 / 2$ .

Therefore positronium formation is forbidden, if the electron and positron affinities are too large. This is the case for example in metals, where the binding energy of the positron is significantly below 6.8 eV, because of the high electron density in the conduction band. Therefore the annihilation of  $e^+e^-$  pairs in aluminum or copper does not occur through positronium, but through spontaneously decaying states.

## 2.2 The $^3S \rightarrow ^1S$ conversion

If the positronium formation in a medium is possible, the singlet state forms on average in 25 % of the cases, and the triplet state in 75 % of the cases, because of the three-fold degeneracy of the  $^3S$  state. The lifetime spectrum is therefore influenced by the following processes:

1. spontaneous decay of positrons which do not form positronium; as discussed in section 1, the decay predominantly produces 2  $\gamma$  quanta
2. decay of the singlet state with a short lifetime (see task 3)
3. decay of the triplet state with a longer lifetime (see task 3)

The latter, however, does not decay with the long lifetime as calculated in task 3, but significantly faster. This is caused by the conversion of the  $^3S$  into the  $^1S$  state, which is possible in solid matter with variable mean conversion time [7]<sup>7</sup>.

The most probable process for the conversion is the exchange of the electron caused by a collision of the positronium with an electron in the medium. Here the exchanged electron takes, together with the positron, the energetically preferred  $^1S$  state. Less likely is a spin flip from the  $^3S$  state into the  $^1S$  state through magnetic interaction during a collision. This spin flip becomes significant, if a strong external magnetic field is applied.

## 3 Experimental setup

### 3.1 Source and detector

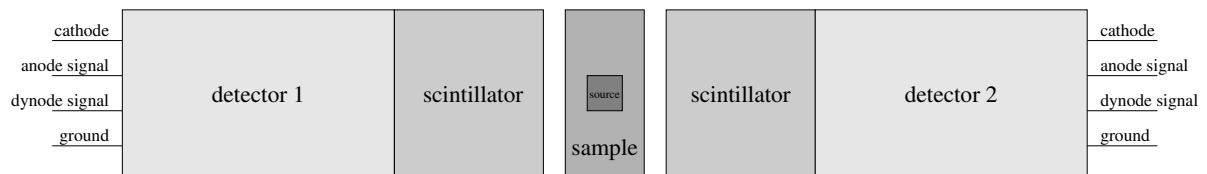


Figure 3: Arrangement of the detectors around the source

A suitable positron source is  $^{22}\text{Na}$  with a maximum positron energy of 540 keV. The decay of  $^{22}\text{Na}$  virtually happens only through the first excited state of  $^{22}\text{Ne}$ , which spontaneously transits to the ground state through irradiation of a 1.28 MeV  $\gamma$  quantum (see Figure 7). This property of the source enables one to use a time spectrometer for the detection of the positrons. For this, two detectors face each other on both sides of a source, which is embedded in mater such that all positrons are stopped in the coating (see Figure 3). One of the detectors is set up to detect the 1.28 MeV  $\gamma$  quanta and provides the start signal, some time later the second detector registers one of the photons<sup>8</sup> from the annihilation of the positron with an electron and provides the stop signal for the time spectrometer. The measured time difference is converted to a pulse with a height proportional to the time difference. The measured time spectrum then corresponds to a spectrum of pulse heights, which is depicted in Figure 5. This pulse height spectrum can be measured with a multi channel analyzer (MCA).

The possible activity of the source is limited by the allowed number of random coincidences, the background in this measurement.

The number  $dn_i$  of real coincidences per time interval  $dt$  in the time bin  $i$ , at which the 1.28 MeV  $\gamma$  and one of the corresponding annihilation photons are measured, is obviously given by:

<sup>7</sup>The conversion in the opposite direction is also possible and discussed in [3].

<sup>8</sup>The possible energies were discussed in Exercise 1. Exercise 2 and Section 2.2 give information on the energies which are to be expected.

$$\frac{dn_{s,i}}{dt} = P_i A \left( \frac{\Omega_1}{4\pi} \right) \epsilon_1 \left( \frac{\Omega_2}{4\pi} \right) \epsilon_2, \quad (19)$$

with  $A$  activity of the source  
 $\Omega_1, \Omega_2$  solid angle covered by the corresponding detector  
 $P_i$  probability for the given time delay in bin  $i$ ,  
i.e. the fraction of events in the time channel  $i$  of the time spectrometer  
 $\epsilon_1, \epsilon_2$  detection efficiency of the detectors

The number of random coincidences per time intervals is:

$$\frac{dn_{c,i}}{dt} = \Delta t A^2 \left( \frac{\Omega_1}{4\pi} \right) \epsilon_1 \left( \frac{\Omega_2}{4\pi} \right) \epsilon_2, \quad (20)$$

where  $\Delta t$  is the width of one time channel. The ratio of both numbers is independent of the detection efficiency and geometry of the setup:

$$a_m = \frac{dn_{c,m}/dt}{dn_{s,m}/dt} = \frac{A \Delta t}{P_m} \quad (21)$$

**Task 4:** A 3 MBq  $^{22}\text{Na}$  source is used. Calculate the relative fraction of the background in the time channel with the highest counting rate. Assume  $P_m = 0.2$  and  $\Delta t = 0.5$  ns.

**Task 5:** Calculate the minimum thickness of the samples to stop the positrons in aluminum and in polyethylene. The density of polyethylene is  $\rho_{PE} = 0.92$  g/cm<sup>3</sup>, that of aluminum is  $\rho_{Al} = 2.70$  g/cm<sup>3</sup>. According to [4] the range  $R_0 = \frac{R}{\rho}$  of  $\beta$  radiation depends on the maximum energy  $E_{\max}$  of the  $\beta$  spectrum and is given by the following empirical relations (the range of positrons differs by up to 10 % from that of electrons):

$$\begin{aligned} R \text{ [g/cm}^2\text{]} &= 0.412 \cdot E_{\max}^n \text{ [MeV]} && 0.01 \text{ MeV} < E_{\max} < 3 \text{ MeV} \\ &\text{with } n = 1.265 - 0.0954 \cdot \ln E_{\max} \text{ [MeV]} \\ R \text{ [mg/cm}^2\text{]} &= 0.0067 \cdot E_{\max}^{1.67} \text{ [keV]} && E_{\max} < 200 \text{ keV} \\ E_{\max} \text{ [MeV]} &= 1.92 \sqrt{R^2 + 0.22R}, \quad [R] = \text{g/cm}^2 && E_{\max} < 700 \text{ keV} \\ R \text{ [g/cm}^2\text{]} &= 0.571 \cdot E_{\max} \text{ [MeV]} - 0.161 && 0.7 \text{ MeV} < E_{\max} < 3 \text{ MeV} \\ R \text{ [g/cm}^2\text{]} &= 0.53 \cdot E_{\max} \text{ [MeV]} - 0.106 && 1 \text{ MeV} < E_{\max} < 20 \text{ MeV} \end{aligned}$$

The expected time differences are in the order of nanoseconds and less. Thus, the detectors have to be able to deliver very short pulses. These specifications are only fulfilled by scintillation counters with plastic scintillators. The excitation of these scintillators has a decay time of around 1–2 ns with deviations of around 0.1 ns. However, they have the disadvantages of a low light yields and mediocre quantum efficiencies.  $\gamma$  quanta of the used energies are only detected through the Compton effect in the scintillator<sup>9</sup>. The detectors are equipped with fast photomultiplier tubes (PMTs) with twelve stages and two outputs each (anode and last dynode) for 50  $\Omega$  coaxial cables. The transit time jitter of the electrons in the tube is less than 1 ns, according to the manufacturer.

### 3.2 The time spectrometer

The time spectrometer is divided into a fast and a slow circuit, called “fast-slow-coincidence”. The fast circuit produces the information on the time difference between the start and the stop signal, while the slow circuit performs the event selection, to record only signals with the correct photon energies.

**Task 6:** What is the difference between the anode and dynode outputs of the scintillation counters in figure 3 (see also the circuit diagram of the voltage divider in figure 6)? Which output is better suited for the time measurement and which for the energy selection? Why are two different outputs used and not a simple T-piece?

<sup>9</sup>see [1, chapter 7.7.3] and Compton edge in [9]



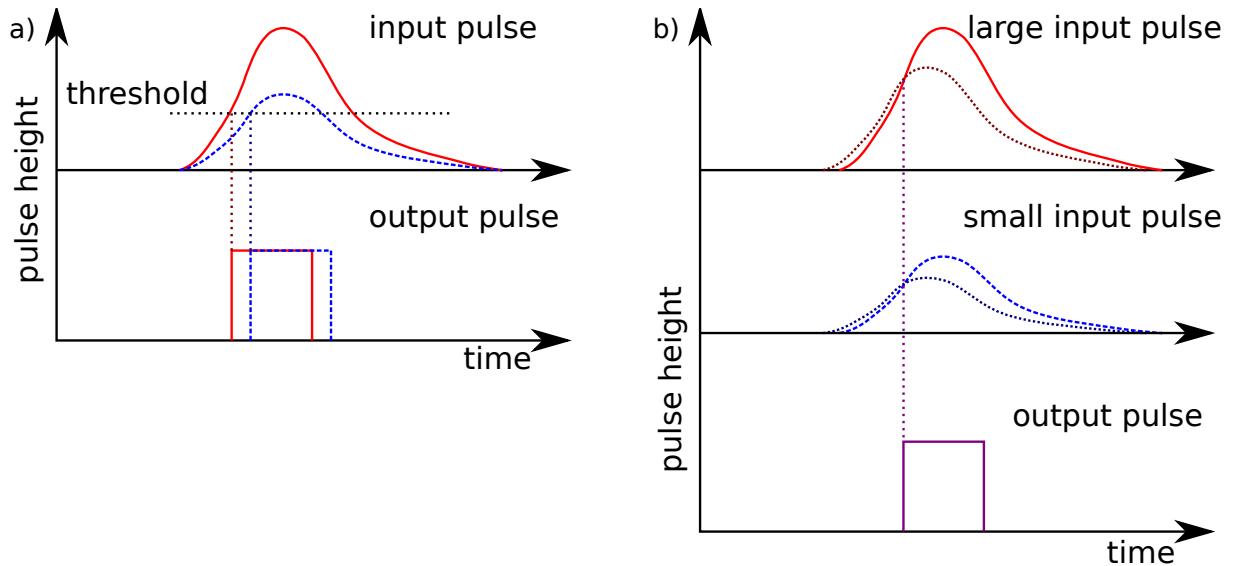


Figure 4: Production of a signal with stable timing in a constant fraction discriminator

In the fast circuit, the pulses of both photomultipliers are first processed with two fast discriminators, to prevent the noise of the PMTs from entering the following read out components and to define upper limits for the pulses. The output pulses of comparators<sup>10</sup> normally suffer from time jitter, which depends on the pulse height spread of the input pulses. This so-called “time walk” effect is illustrated in figure 4a. To prevent this effect from happening, constant fraction discriminators (CFD) are used, which produce time marks on the same relative position of the rising edge of pulses, if these have a constant rise time. In the used CFDs, the input signal is compared to an amplified and delayed copy of itself. The crossing of these two copies of the signal always happens at the same time relative to the peak of the pulse. This is illustrated in figure 4b.

The following electronic circuit consist of the time-to-amplitude converter (TAC), which does the following: The starting pulse enables a constant current source, which charges a capacitor until the stop signal is detected. Afterwards the capacitor is discharged through a resistor. This gives a voltage pulse, with a height proportional to the time difference between the start and the stop signal. The output of the TAC is connected to the input of the MCA, so that a spectrum of pulse heights is recorded.

The slow coincidence circuit is used for the energy selection of the start and stop signals. Both photomultipliers provide an additional output signal for this. The signals are fed into an amplifier-analyzer unit and are analyzed with standard one-channel window discriminators. In the start branch only the 1.28 MeV  $\gamma$  quanta, in the stop branch only the photons from the annihilation pass. The outputs of both discriminators are coupled through a coincidence with a time window of about 1  $\mu$ s. The output of the coincidence stage is used as a gate signal for the MCA, so that it can detect the time signal from the TAC.

**Task 7:** Conceive a block diagram of the time spectrometer with slow and fast circuit, using the description above and the device list in section A.1.

### 3.3 Operating point and calibration of the setup

When a time signal reaches the MCA, the gate must already be open. Because the time signal is faster than the corresponding gate signal, it has to be delayed by a linear delay unit. With a two channel oscilloscope the timing of both signals can be checked visually.

The calibration of the relation between time difference and pulse height (or channel number of the MCA) can be done by an additional variable delay in the stop branch of the TAC. The relation should be linear and is measured in ns/channel. The resolution  $\Delta t$  is defined as the width of the pulse height distribution for events with a vanishing (or constant) time difference. Here the pure electronic and the total time resolution of the spectrometer can be distinguished. The pure electronic time resolution is a property of just the fast circuit and is used to test its

<sup>10</sup>often called “level discriminators”

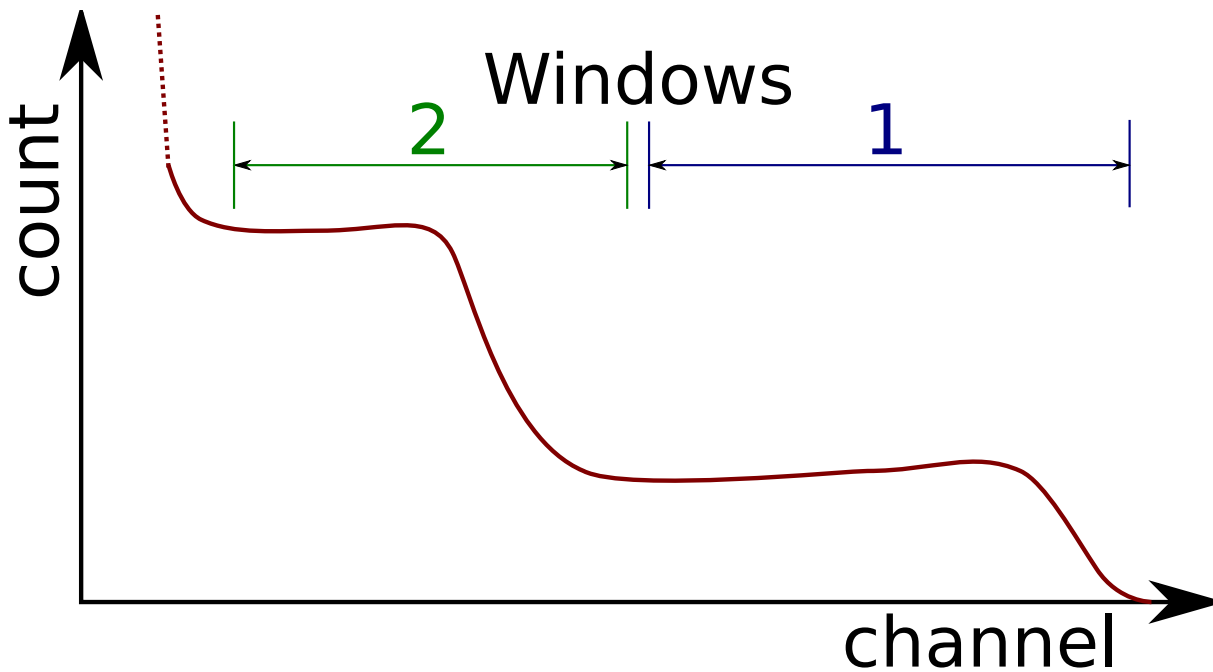


Figure 5: Pulse height spectrum of the  $\gamma$  quanta from the decay of  $^{22}\text{Na}$ , recorded with a plastic scintillator

functionality. It is measured by replacing the detectors by a fast pulse generator with two synchronous outputs. The gate of the MCA is not used. For the measurement of the total time resolution of the detector, including detectors and the slow circuit,  $^{60}\text{Co}$  can be used. According to the decay scheme (see Figure 8) the decay cascade from  $^{60}\text{Co}$  to  $^{60}\text{Ni}$  produces two nearly instantaneous  $\gamma$  quanta<sup>11</sup> with energies of 1.17 MeV and 1.33 MeV and only weak directional correlation.

To adjust the energy windows for the slow circuit, the amplified PMT signal (instead of the TAC output) is used as an input to the MCA, and therefore an energy spectrum is recorded. The gate of the MCA is driven by the output of the discriminator which is adjusted. The position of the thresholds can then be seen as cuts in the energy spectrum of the MCA. A proper length and timing of the gate and the signal has to be ensured by the use of delay stages and gate generators. The selection of the energy windows for the slow circuit is illustrated in figure 5. The diagram shows the pulse height spectrum of one of the scintillation counters, which is produced by a superposition of the spectra of the Compton electrons in the plastic scintillator, caused by the 1.28 MeV  $\gamma$  quanta and the annihilation photons.

## 4 Analysis of the time spectra

The analysis of the time spectra is difficult for two reasons:

1. It is possible, that the time spectrum is a superposition of spectra with more than one time constant. In polyethylene the long time constant of the  $^3S \rightarrow ^1S$  conversion is well separated from the short time constant of spontaneous decay. In aluminum only decays with one short time constant occur, as long as the material is sufficiently pure.

2. The time resolution of the setup can be in the same order of magnitude as the lifetime to be measured, so that the measured spectrum is a convolution of the real decay time spectrum and the resolution function. In this case the measured curve has to be either deconvoluted, or a fitting approximate method has to be used. For this two methods are suitable:

<sup>11</sup> $\Delta t < 10^{-12}$  s

## 4.1 The “tail” method

The “tail” method is suitable for lifetimes greater than the total time resolution, when the latter can not be neglected. Be  $F(t)$  the measured time spectrum<sup>12</sup>,  $P(t)$  the time resolution measured with  $^{60}\text{Co}$ , and  $f(t)$  the true time spectrum of the decay. Then  $F(t)$  is produced by a convolution integral:

$$F(t) = \int_{-\infty}^{\infty} f(T) P(t - T) dT \quad (22)$$

As a decay process,  $f(t)$  follows a (normalized) exponential function:

$$f(t) = \begin{cases} \lambda e^{-\lambda t} & \text{for } t \geq 0 \\ 0 & \text{otherwise} \end{cases} \quad (23)$$

From this follows:

$$F(t) = \lambda \int_0^{\infty} e^{-\lambda T} P(t - T) dT \quad (24)$$

With the substitution  $y = t - T$  one can deduce:

$$F(t) = \lambda e^{-\lambda t} \int_{-\infty}^t e^{\lambda y} P(y) dy \quad (25)$$

Differentiation of the equation produces:

$$\frac{dF(t)}{dt} = \lambda (P(t) - F(t)) \quad (26)$$

$$\Rightarrow \frac{d}{dt} \ln F(t) = \frac{\frac{dF(t)}{dt}}{F(t)} = -\lambda \left( 1 - \frac{P(t)}{F(t)} \right) \quad (27)$$

Equation 26 shows, that the maximum of the measured curve  $F(t)$  is located exactly in the intersection point with the resolution curve  $P(t)$ , when both curves are normalized to the same number of events. Equation 27 can be used directly for the analysis of the data to determine  $\lambda$ . If there is enough data in a longer time range where  $P(t) \ll F(t)$ , it is possible to use an approximation:

$$\frac{d}{dt} \ln F(t) \approx -\lambda \quad (28)$$

This can be applied through a linear regression in a semilogarithmic representation.

**Task 8:** Verify the calculation from the convolution integral in equations 22 to 28.

## 4.2 The “centroid shift” method

The “centroid shift” method is used, when the lifetime is smaller than the total time resolution. In this case the positron decay is only visible through a broadening of the resolution curve and a small shift to  $t > 0$ . The procedure is based on the determination of the first moments about 0 of the measured time spectrum as well as the resolution curve.

The  $n$ th moment of a function  $g(x)$  is defined as:

$$M^n [g(x)] = \int_{-\infty}^{\infty} x^n g(x) dx \quad (29)$$

As above,  $F(t)$  is the total measured time spectrum,  $P(t)$  the resolution curve, and  $f(t)$  the true time spectrum, as given in equations 22 and 23. Then the following relation between the moments holds [3]:

$$M^n [F(t)] = \sum_{k=0}^n \binom{n}{k} M^{n-k} [P(t)] M^k [f(t)] \quad (30)$$

<sup>12</sup>more precisely: pulse height spectrum

The calculation of the 0th and 1st order moments  $M^0 [F(t)]$ ,  $M^1 [F(t)]$  and  $M^0 [P(t)]$ ,  $M^1 [P(t)]$  then produces the desired lifetime:

$$\tau = \frac{1}{\lambda} = \frac{M^1 [F(t)]}{M^0 [F(t)]} - \frac{M^1 [P(t)]}{M^0 [P(t)]} \quad (31)$$

Transferred to channel numbers this gives:

$$\tau = \frac{1}{\lambda} = \left( \frac{\sum_i t_i N_{F,i}}{N_{F,tot}} - \frac{\sum_i t_i N_{P,i}}{N_{P,tot}} \right) \Delta t \quad (32)$$

with  $\Delta t$  time width of one channel  
 $t_i$  channel number  
 $N_{F,i}$  count in channel  $t_i$  of the time spectrum  $F(t)$   
 $N_{P,i}$  count in channel  $t_i$  of the resolution curve  $P(t)$   
 $N_{X,tot} = \sum_i N_{X,i}$  total event count of the curve  $X$

Obviously the terms in parentheses are the centroids of both distributions  $\bar{t}_X = (\sum_i t_i N_{X,i}) / N_{X,tot}$ . That means:

$$\tau = (\bar{t}_F - \bar{t}_P) \Delta t \quad (33)$$

The lifetime is proportional to the shift of the centroid of the distribution. The standard deviation of the centroid is:

$$\sigma_{t,X} = \sqrt{\frac{\sum_i (t_i - \bar{t}_X)^2 N_{X,i}}{N_{X,tot} - 1}} \quad (34)$$

The mean uncertainty on the centroid is:

$$\sigma_{m,X} = \sqrt{\frac{\sum_i (t_i - \bar{t}_X)^2 N_{X,i}}{N_{X,tot} (N_{X,tot} - 1)}} = \frac{\sigma_{t,X}}{\sqrt{N_{X,tot}}} \quad (35)$$

The total statistical uncertainty of the centroid shift is then given by:

$$\sigma = \sqrt{\sigma_{m,F}^2 + \sigma_{m,P}^2} \quad (36)$$

**Task 9:** Verify equation 31 and the transition to the binned equation 32.

## 5 Experimental procedure

Before the experiment, it is advisable to first solve the tasks in this manual, as they consider all the important aspects. Record all settings chosen while performing the experiment.

### 5.1 Setting up, adjusting of the operating point and calibration

1. Putting the scintillation counters into operation:

Place a  $^{22}\text{Na}$  sample between the detectors. Slowly increase the high voltage of the PMTs. Monitor the anode signal with an oscilloscope while ramping. Try to limit the signal amplitude to the maximum allowed voltage of the other modules in the signal chain. Check the specifications in the documentation of each module. Characterize and sketch the signals while noting amplitude, rise and fall times.

2. Adjusting the pulse height windows in the slow circuit:

Set up the slow circuit to test the window setup of the discriminators. For the window adjustment it is advisable to record the pulse height spectrum of the amplifier output with the MCA (as seen in figure 5). Here it is important to mind the polarity of the signals. When the MCA is gated by the discriminator output of the amplifier-analyzer unit, only the selected part of the spectrum (with steep edges) is plotted. Because the discriminator signal only arrives some microseconds after the amplifier output, both signals have to be temporally adjusted through a delay. Here the time walk effect of the discriminator as illustrated in figure 4a has to be taken into account.

### 3. Tuning of the fast circuit:

Set up the fast circuit. Adjust the fast discriminators such, that the threshold for the start pulses coincides with the upper end of the Compton spectrum of the annihilation photons, and that with the threshold for the stop pulses the biggest part of the noise is suppressed. The settings can be verified with the MCA or with an oscilloscope triggered by the corresponding discriminator output.

### 4. Verification of the linearity of the time-pulse height conversion and time calibration:

Replace both detectors by a pulse generator. Pulse height and pulse width should be in the same order of magnitude as the detector signals. Send the TAC output signals into the MCA while disabling the gate. Verify the linearity between time and pulse height over a range of 0 ns to about 10–15 ns. An adjustable ns-delay unit can be used in the stop branch to achieve this. The time-pulse height relation<sup>13</sup> can also be used to obtain the time calibration of the spectrometer<sup>14</sup>, which is used in the analysis of the following measurements. Verify that the pure electronic time resolution  $\Delta t$  of the spectrometer<sup>15</sup> is smaller than 50 ps. Choose the range of the TAC according to the needs of the further measurements. The delay in the stop circuit should be set to some small value for the further measurements. If the lowest part of the time spectrum shows a non-linearity, the delay should be used to shift the measured time spectrum into the region of linearity.

### 5. Verification of the total time spectrum:

Assemble the complete time spectrometer and place the  $^{60}\text{Co}$  source between the detectors.  $^{60}\text{Co}$  produces two virtually instantaneous photons per decay. Check the time delay between signal pulse (from the TAC) and gate of the MCA on an oscilloscope and adjust it if needed. The  $^{60}\text{Co}$  signal does not have to be at the exact same place  $t = 0$  as the signal of the pulse generator<sup>16</sup>, but not far away. Make sure the discriminator thresholds that were tuned for  $^{22}\text{Na}$  are suitable for the measurements with  $^{60}\text{Co}$ .

Do some fast measurements with the  $^{22}\text{Na}$  samples to verify that the measurement range is sufficient. If the range is changed, the time calibration with the pulse generator has to be redone.

## 5.2 Measurement series

Make sure the delay in the stop branch is set to a suitable value before starting the measurements. Each series of measurement should have at least 10 000 events. If possible, try to collect more events using a longer run time.

#### 1. $^{60}\text{Co}$ :

The two instantaneous  $\gamma$  quanta produce the experimental resolution curve. The time resolution (width at half maximum  $\Delta t$ ) should be around 500 ps and not greater than 700 ps.

#### 2. $^{22}\text{Na}$ in aluminum:

It should be visible already in the spectrum displayed by the MCA, that the spectrum is broadened compared to the resolution curve. Compare the position of the maximum with that of the resolution curve. An early estimate of the lifetime can be made to ensure that it is roughly as expected.

#### 3. $^{22}\text{Na}$ in polyethylene:

This spectrum should use a much wider time range. Make sure that enough background through random coincidences is measured, and that the long tail at large times contains enough events to determine the long lived component.

#### 4. $^{60}\text{Co}$ :

To test the stability of the setup, repeat the measurement with  $^{60}\text{Co}$  at the end.

---

<sup>13</sup>delay vs. channel number

<sup>14</sup>channel width in time units

<sup>15</sup>standard deviation of the distribution on the MCA

<sup>16</sup>Why not?

## 6 Analysis and report

Take into account error propagation in all calculations, or give reasons why it can be neglected. If you use  $\chi^2$  fits for the analysis, ensure that the values of  $\chi^2$  are sensible. If you make a fit to only part of the curves, test the stability of the result when varying the borders of the fit range. How can this be considered for the estimation of the uncertainties?

The analysis should at least include the following points:

1. Plot the time-channel number curve that was generated with the help of the pulse generator and check the linearity. Determine the time calibration (channel width in ps, including the uncertainty).
2. Determine the background for all recorded spectra, using a suitable time range<sup>17</sup> of the curves.
3. Plot both <sup>60</sup>Co resolution curves after a background subtraction. Determine the mean including uncertainty and the experimental time resolution. Compare both measurements and comment on the time stability of the setup.
4. Plot the normalized time spectrum of the positron decay in aluminum after a background subtraction together with the normalized resolution curve. Make sure to do the normalization after the background subtraction. Use a suitable analysis method to determine the lifetime of the positrons.
5. Plot the normalized time spectrum of the positron decay in polyethylene after a background subtraction together with the normalized resolution curve. You might want to rebin<sup>18</sup> the histogram if there are too few events per bin, perhaps even with variable bin width<sup>19</sup>. Check whether the measured curve intersects the resolution curve at its maximum, to justify the tail method. Determine the lifetimes of the para-positronium and the ortho-positronium using the tail method. It might be sufficient to use only the linear part of the spectrum in a semilogarithmic plot. Determine the ratio between para-positronium and converted ortho-positronium.
6. Discuss the results and compare them with the expectation.

## A Devices and material

### A.1 Devices

- 2 photomultiplier tubes, Valvo type XP1020, circuit diagram see figure 6, each with one piece of plastic scintillator 20 mm, length 10 mm, operating voltage around –1900 V
- 1 two-channel high voltage module, CAEN, model N471
- 1 time analyzer, Canberra, model 2043
- 2 amplifier analyzer (with coincidence unit), Nuclear Enterprises, model 4630
- 1 delay unit 0.5–63.5 ns, SEN, model FE 290
- 1 quad gate/delay generator, Phillips Scientific, model 794
- 1 multi channel analyzer, Multitport II, Canberra
- 1 pulse generator, four channel digital delay/pulse generator, Stanford Research Systems Inc., model DG535
- 1 digital oscilloscope
- 2 delay amplifier, Canberra, model 1457
- 2 constant fraction discriminator, CMTE, model 7029A
- 1 dual linear amplifier, LRS, model 133B
- 1 PC for the readout of the MCA

---

<sup>17</sup>Where is only noise present?

<sup>18</sup>Reduce the number of bins by combining multiple bins.

<sup>19</sup>take care when determining the errors

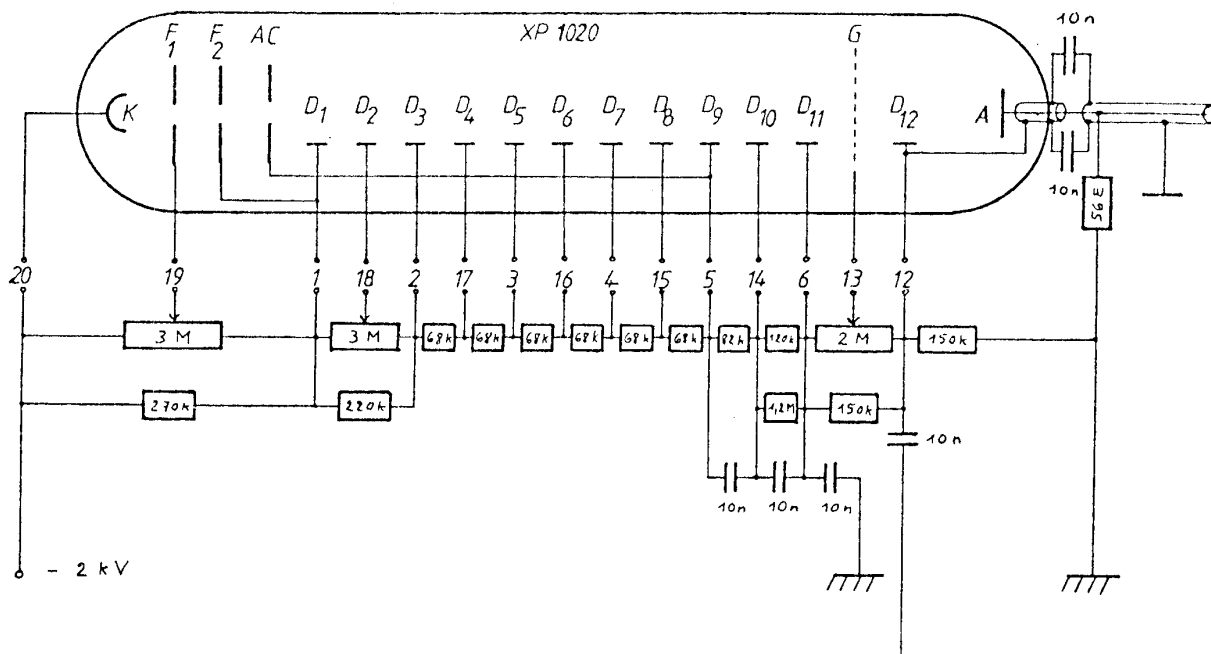


Figure 6: circuit diagram for the voltage divider of the PMT XP1020

## A.2 Material

- 1  $^{60}\text{Co}$  preparation no. MW 970, 282.29 kBq on 2006-12-31, embedded between two slices of polyethylene, each 85 mm  $\varnothing$  and 4 mm thick
- 1  $^{22}\text{Na}$  preparation no. SV 283, 3.43 MBq on 2010-07-01, embedded between two slices of aluminum, each 85 mm  $\varnothing$  and 4 mm thick
- 1  $^{22}\text{Na}$  preparation no. SV 284, 3.39 MBq on 2010-07-01, embedded between two slices of polyethylene, each 85 mm  $\varnothing$  and 4 mm thick

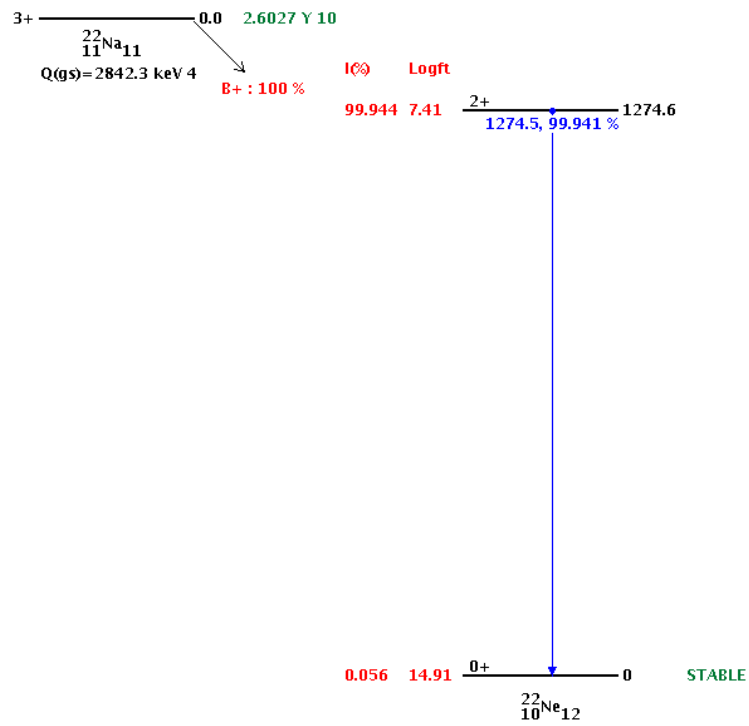


Figure 7: Decay scheme of  $^{22}\text{Na}$ . Source: [5]

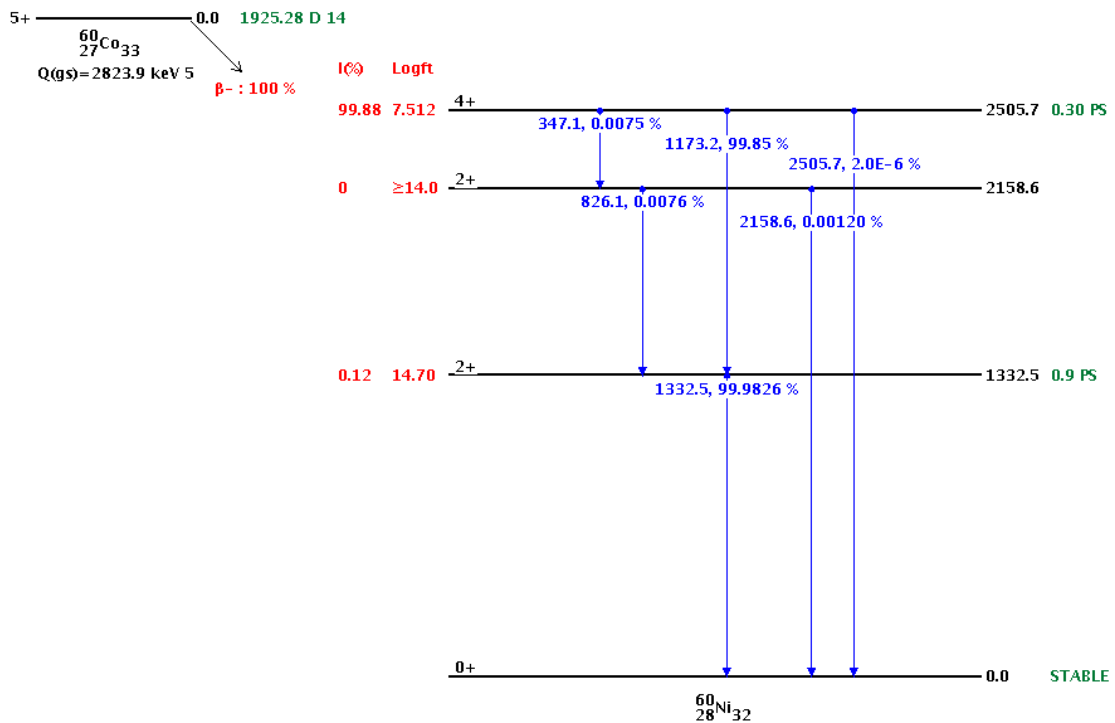


Figure 8: Decay scheme of  $^{60}\text{Co}$ . Source: [5]